Inorganic Chemistry

Article

pubs.acs.org/IC

Cation Exchange in a 3D Perovskite—Synthesis of $Ni_{0.5}TaO_3$

Midori Amano Patino,[†] Thomas Smith,[†] Weiguo Zhang,[‡] P. Shiv Halasyamani,[‡] and Michael A. Hayward*[,†]

[†]Department of Chemistry, University of Oxford, Inorganic Chemistry Laboratory, South Parks Road, Oxford OX1 3QR, United Kingdom

[‡]Department of Chemistry, University of Houston, 112 Fleming Building, Houston, Texas 77204-5003, United States

Supporting Information

ABSTRACT: Reaction of $NiCl_2$ with $NaTaO_3$ leads the formation of the perovskite phase $Ni_{0.5}TaO_3$, via a topochemical nickel-for-sodium cation exchange in which the framework of apex-linked TaO_6 octahedra present in the parent phase is retained. Neutron powder diffraction data indicate $Ni_{0.5}TaO_3$ adopts a structure analogous to the paraelectric phase of $LiTaO_3$, with triclinic $P\bar{1}$ crystallographic symmetry. Although $Ni_{0.5}TaO_3$ has features which make it a good candidate phase for magnetoelectric multiferroic behavior, the phase remains paramagnetic in the temperature range $15 < T\,(K) < 300$, and detailed crystallographic characterization and analysis of SHG activity indicate it retains a centrosymmetric structure down to the lowest temperatures measured (5 K). Topochemical cation exchange reactions of 3D perovskite oxides offer the opportunity to prepare a wide range of novel metastable phases in a rational manner with a high degree of synthetic control.

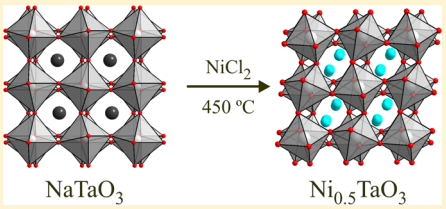

INTRODUCTION

The preparation of materials which exhibit magnetoelectric multiferroic behavior is extremely challenging because, as pointed out by Spaldin (née Hill), the constituent properties—ferroelectricity and (ferro)magnetism—are contraindicated.[1] This contraindication can be understood by observing that it is only possible for a phase to exhibit a net spontaneous electric polarization if it has a noncentrosymmetric structure. However, given the thermodynamic favorability of regular packing arrangements, particularly in extended oxides, unless specific measures are taken to break structural inversion symmetry, the vast majority of oxide phases will adopt centrosymmetric structures.[2]

The conventional approach used to overcome the inherent favorability of centrosymmetric packing in oxide systems, exploits electronically driven structural distortions (typically based on a second order Jahn−Teller (SOJT) instability) to break the local inversion symmetry of structures. This is usually achieved in one of two ways: (i) by including octahedrally coordinated d^0 transition metal cations (e.g., Ti^{4+}, Ta^{5+}, W^{6+}) which are susceptible to a SOJT distortion in which the metal d orbitals hybridize with the oxygen 2p orbitals, driving a spontaneous "off-centering" of metals within their anion coordination polyhedra.[3−7] (ii) by including post-transition metal "lone-pair" cations with ns^2 electronic configurations (e.g., Pb^{2+}, Bi^{3+}), which hybridize their s and p orbitals orbitals with the oxygen 2p orbitals driving a structural distortion (often interpreted as a "lone-pair" at the metal center) which breaks the symmetry of the metal−anion coordination polyhedra.[8−13] By harnessing these structural distortions, ferroelectric materials can be prepared semirationally, however d^0 transition metals and ns^2 post-transition metals are diamagnetic, thus ferroelectric materials prepared via this strategy will also tend to be diamagnetic, hence the observed contraindication of ferroelectricity and magnetism.[1]

In order to introduce magnetism into ferroelectric materials, either some other symmetry breaking mechanism must be employed or a "composite" strategy making use of a combination of paramagnetic cations and diamagnetic symmetry-breaking cations must be adopted. This composite strategy has been used widely in ABO_3 cubic perovskite phases. By locating paramagnetic transition metal cations in the octahedral B-sites, a strongly interacting array of magnetic centers can be formed, while locating nonspherical, ns^2 post-transition metal cations on the 12-coordinate A-site tends to break the inversion symmetry of the perovskite lattice, fulfilling both prerequisites for magnetoelectric behavior. By following this strategy, a number of interesting candidate phases for coupled magnetoelectric behavior have been prepared;[14−17] however, many perovskite phases with large A-site cations such as Pb^{2+} or Bi^{3+} are unstable at ambient pressure and require complex high pressure syntheses, limiting this approach.

The alternative composite magnetoelectric perovskite formulation, with symmetry-breaking d^0 transition-metal B-site cations and paramagnetic A-site cations, has not been widely explored as the lack of suitably large, paramagnetic monovalent or divalent cations suggests any perovskite phase in this class would not be thermodynamically stable. Topochemical cation exchange reactions offer the opportunity to prepare metastable phases by substituting large diamagnetic cations (Na^+, K^+, Rb^+, Cs^+) with smaller paramagnetic ions

Received: April 14, 2014
Published: July 22, 2014

   dx.doi.org/10.1021/ic500881v | Inorg. Chem. 2014, 53, 8020−8024

such as Co^{2+}, Ni^{2+}, or Cu^{2+}.[18−20] For example, reaction of the Ruddlesden−Popper phase $Na_2La_2Ti_3O_{10}$ with mixtures of $CoCl_2$/KCl or $CuCl_2$/KCl leads to a cation exchange in which two Na^+ cations are replaced by a single Co^{2+} or Cu^{2+} cation forming $CoLa_2Ti_3O_{10}$ or $CuLa_2Ti_3O_{10}$ respectively, with retention of the Ti−O framework of the parent $Na_2La_2Ti_3O_{10}$ phase.[21]

In pursuit of a magnetic A-site, symmetry-breaking B-site, multiferroic material we have turned our attention to the cation exchange chemistry of 3D perovskite phases containing monovalent A-site cations. Here we report the nickel-for-sodium cation exchange chemistry of the perovskite phase $NaTaO_3$.

EXPERIMENTAL SECTION

Synthesis of $NaTaO_3$. Samples of $NaTaO_3$ were prepared via a ceramic route. A 1:1 molar ratio of Na_2CO_3 (99.997%) and Ta_2O_5 (99.993%, dried at 900 °C) were thoroughly mixed in an agate pestle and mortar and then heated in air at 900 °C to decompose the carbonate. The resulting mixture was then reground and pressed into 13 mm pellets and then heated for 2 periods of 24 h at 1000 °C in air, with intermediate regrinding. The resulting material was observed to be a single phase by X-ray powder diffraction, with lattice parameters (spacegroup: *Pcmn*, a = 5.525(1) Å; b = 7.794(1) Å; c = 5.480(1) Å) in good agreement with published values.[22]

Preparation of $Na_{1-2x}Ni_xTaO_3$. Cation exchange reactions were performed by reacting $NaTaO_3$ with $NiCl_2$ (99.95%, dried at 280 °C as detailed in the Supporting Information). To investigate the reactivity of the system, 10:1 molar ratios of $NiCl_2/NaTaO_3$ with a total mass of ∼2g were ground together in an argon-filled glovebox, sealed in evacuated silica ampules, and then heated at temperatures between 400 and 500 °C, with intermediate regrinding and resealing as required. After reaction, NaCl produced in the reaction and excess $NiCl_2$ were removed from samples by washing in 1.2 M HCl and then distilled water. Products were then filtered and dried in air at 75 °C. Caution: heating of incompletely dried $NiCl_2$ in sealed ampules is an explosion hazard.

Samples for analysis by neutron powder diffraction were prepared by heating 10:1 molar ratios of $NiCl_2/NaTaO_3$ (based on a mass of 5g $NaTaO_3$) at 450 °C for 6 periods of 7 days. Samples were then washed in 1.2 M HCl and then distilled water before being dried in air at 75 °C.

Characterization. X-ray powder diffraction data were collected using a PANalytical X'Pert diffractometer incorporating an X'celerator position-sensitive detector (monochromatic Cu Kα1 radiation). Prior to the final washing step, samples were measured in gastight sample holders due to the deliquescence of $NiCl_2$. Neutron powder diffraction data were collected from samples contained within vanadium cans using the D2B instrument (λ = 1.594 Å) at the ILL neutron source, Grenoble. Rietveld profile refinements were performed using the GSAS suite of programs.[23] Magnetization data were collected using a Quantum Design MPMS SQUID magnetometer. Powder second harmonic generation (SHG) measurements were performed using a modified Kurtz-NLO system[24,25] incorporating a pulsed Nd:YAG laser with a wavelength of 1064 nm. The equipment and methodology has been described in detail previously.[26]

RESULTS

X-ray powder diffraction data collected from reaction mixtures heated at 400 °C showed no evidence of reaction; however, mixtures heated at 450 °C showed a very slow transformation, over a period of weeks, from orthorhombic $NaTaO_3$ to a new material which could be approximately indexed using a rhombohedral cell, as shown in Figure 1. Samples became paramagnetic with moments that increased as the transformation progressed (excess $NiCl_2$ was removed prior to magnetic measurement by washing in dilute HCl) and weak,

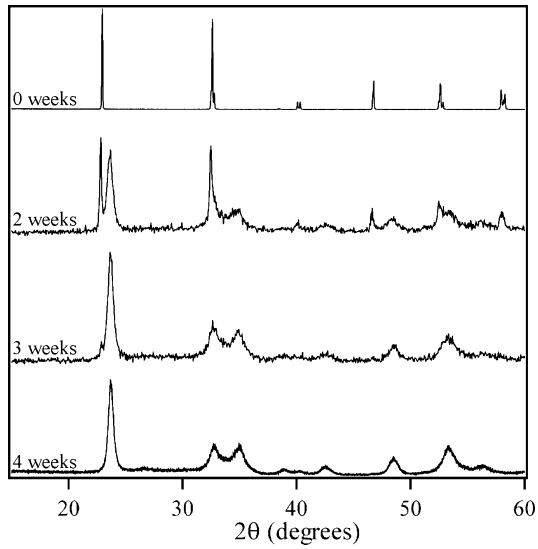

Figure 1. X-ray powder diffraction patterns collected from reactions between $NaTaO_3$ and $NiCl_2$ at 450 °C, as a function of reaction time. Samples have been washed to remove excess $NiCl_2$.

broad diffraction peaks attributable to NaCl were observed in the X-ray powder patterns collected from unwashed reaction products. These observations are consistent with the cation exchange reaction described in reaction 1.

$$NaTaO_3 + 1/2NiCl_2 \rightarrow Ni_{0.5}TaO_3 + NaCl \quad (1)$$

Reaction mixtures heated at 500 °C rapidly yielded $NiTa_2O_6$, a cation ordered rutile phase previously prepared via high-temperature synthesis routes and presumed to be the thermodynamically most stable $Ni_xTa_{2x}O_{6x}$ phase.[27]

X-ray and neutron powder diffraction data collected at room temperature from a reaction mixture heated for 4 periods of 1 week, with intermediate regrinding, and then washed in dilute acid (henceforth referred to as $Ni_{0.5}TaO_3$) could be approximately indexed by a rhombohedral cell (a = 5.48 Å, α = 55.73°) similar to that reported for the high-temperature paraelectric phase of $LiTaO_3$.[28] Therefore, a structural model based on $LiTaO_3$, but with each lithium atom replaced by 0.5 Ni atoms, was refined against the neutron diffraction data. The refinement proceeded smoothly; however, the fit between the model and the data was very poor (χ^2 = 9.12). Close inspection of the data indicated that the rhombohedral unit cell did not accurately index all the observed diffraction peaks and that the crystallographic symmetry was in fact triclinic (Figure 2). Therefore, a new model was constructed by transposing the atoms from the rhombohedral model into a triclinic cell of the same volume with space group $P\bar{1}$. Refinement of this model against the neutron diffraction data proceeded smoothly and led to a significant improvement to the fit (χ^2 = 4.088). In the final model, thermal displacement parameters were constrained by element to aid refinement stability. Refinement of the nickel site occupancies did not lead to significant deviations from 25% occupation, consistent with the stated $Ni_{0.5}TaO_3$ composition. Observed, calculated and difference plots from the final refinement are shown in Figure 2, with details of the refined model in Table 1. An identical model was refined against analogous neutron powder diffraction data collected from $Ni_{0.5}TaO_3$ at 5 K, as detailed in the Supporting Information.

In order to determine if there is a significant amorphous portion in the sample, X-ray powder diffraction data were

dx.doi.org/10.1021/ic500881v | Inorg. Chem. 2014, 53, 8020−8024

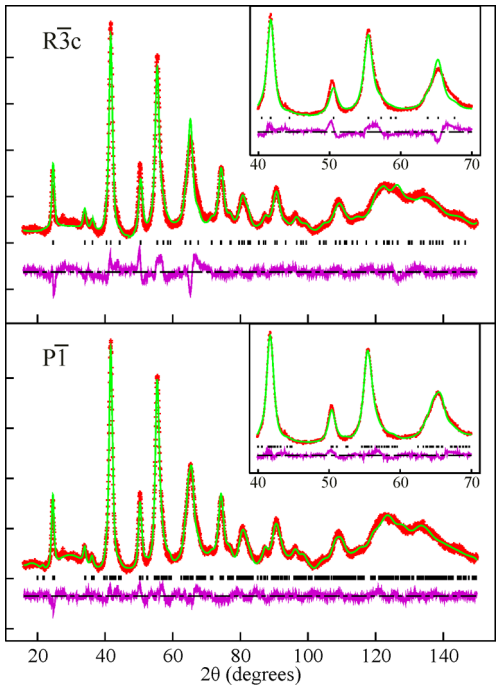

Figure 2. Observed, calculated, and difference plots from the refinement of structural models in space groups $R\bar{3}c$ (top; χ^2 = 9.12) and $P\bar{1}$ (bottom; χ^2 = 4.088) against neutron powder diffraction data collected at 298 K. Insets show expanded region 40 < 2θ (°) < 70.

Table 1. Structure of $Ni_{0.5}TaO_3$ Refined against Neutron Powder Diffraction Data Collected at Room Temperature

atom	x	y	z	fraction	U_{iso} (Å^2)
Ta(1)	0	0	0	1	0.019(1)
Ta(2)	1/2	1/2	1/2	1	0.019(1)
Ni(1)	0.352(4)	0.289(5)	0.288(3)	0.26(1)	0.0056(2)
Ni(2)	0.146(5)	0.231(4)	0.170(5)	0.25(1)	0.0056(2)
O(1)	0.862(2)	0.628(2)	0.284(2)	1	0.0018(6)
O(2)	0.625(2)	0.253(3)	0.867(2)	1	0.0018(6)
O(3)	0.241(2)	0.871(2)	0.624(3)	1	0.0018(6)

$Ni_{0.5}TaO_3$ – space group P-1, a = 5.470(1) Å, b = 5.498(1) Å, c = 5.507(1) Å, α = 55.69(1) °, β = 56.19(1) °, γ = 55.31(1) °, v = 105.5(9) Å^3. χ^2 = 4.088, wR_p = 3.38%, R_p = 2.63%.

collected from a mixture of $Na_{0.5}TaO_3$ and silicon with a 69.84%:30.16% mass ratio (Supporting Information). Refinement of a two-phase model against these data yielded mass fractions of 68.8(2)% $Na_{0.5}TaO_3$ and 31.2(2)% silicon. This indicates a maximum of 4.7% mass percent of the $Na_{0.5}TaO_3$ sample could be amorphous.

Magnetization data collected as a function of temperature (Figure 3) could be fitted to the Curie–Weiss law ($\chi = C/(T-\theta)$) in the temperature range 15 < T (K) < 300 (C = 0.56(1) cm^3 K mol^{-1}, θ = −12.8(4) K). The extracted Curie constant is consistent with the value expected for 0.5 × S = 1 Ni^{2+} centers per formula unit, confirming the stated $Ni_{0.5}TaO_3$ composition.

Tests to evaluate the SHG behavior of $Ni_{0.5}TaO_3$ using 1064 nm incident light could observe no measurable effect, consistent with the refined centrosymmetric structure of the phase.

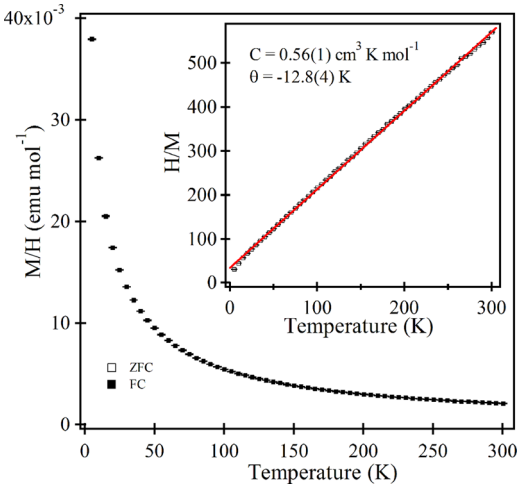

Figure 3. Magnetization data collected from $Ni_{0.5}TaO_3$ in an applied field of 100 Oe. Inset shows fit to the Curie–Weiss law.

DISCUSSION

The X-ray and neutron powder diffraction data show that reaction between $NaTaO_3$ and $NiCl_2$ leads to the formation of the metastable phase $Ni_{0.5}TaO_3$ via a very slow topochemical cation-exchange process in which two Na^+ cations are replaced by a single Ni^{2+} cation, while the apex-linked network of TaO_6 octahedra present in $NaTaO_3$ is conserved. Raising the reaction temperature above 500 °C or annealing washed samples at this temperature, results in the rapid formation of $NiTa_2O_6$, the trirutile, thermodynamically stable form of "$Ni_{0.5}TaO_3$". This suggests that this is the temperature above which the Ta–O framework breaks down and is likely to be the temperature limit for all topochemical reactions involving $ATaO_3$ perovskite frameworks.

The smaller ionic radius of Ni^{2+} compared to Na^+ (Ni^{2+} radius = 0.69 Å; Na^+ radius = 1.02 Å)[29] leads to a large distortion in the Ta–O–Ta framework on cation exchange, in which the rigid TaO_6 octahedra rotate in a cooperative manner to convert the 12-coordinate sodium site present in $NaTaO_3$ into two pseudo-octahedral sites as shown in Figure 4. The resulting framework is analogous to that observed for the paraelectric phase of $LiTaO_3$[28] consistent with the more similar ionic radii of Li^+ and Ni^{2+} (Li^+ radius = 0.76 Å).[29] The major difference between the structure of paraelectric $LiTaO_3$ and $Ni_{0.5}TaO_3$ is that in the former phase the two "octahedral" sites

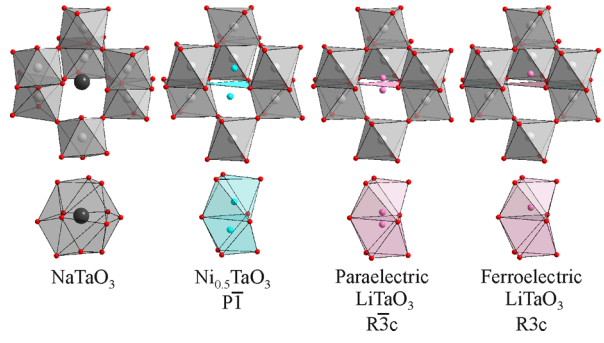

Figure 4. TaO_3 framework and A-cation site(s) of $NaTaO_3$, $Ni_{0.5}TaO_3$, paraelectric and ferroelectric $LiTaO_3$. Gray, black, blue, pink, and red spheres represent tantalum, sodium, nickel, lithium, and oxygen, respectively.

dx.doi.org/10.1021/ic500881v | Inorg. Chem. 2014, 53, 8020–8024

derived from the perovskite A-site are 50% occupied by lithium, whereas in the latter phase, they are 25% occupied by nickel.

The cation exchange reaction leads to a contraction in the lattice volume of 10.5%, a tightening of the Ta−O−Ta bond angles from an average of 159.2° in $NaTaO_3$ to an average of 143.1° in $Ni_{0.5}TaO_3$ and a lowering of the lattice symmetry to triclinic. However, despite the large deformation of the tantalum-oxide lattice, the nickel cations in $Ni_{0.5}TaO_3$ still appear to be "under bonded" with bond valence sums (BVS) of Ni^{+} 1.63 and Ni^{+} 1.56 for the two nickel sites (see Supporting Information)—it should be noted that the lithium cations in paraelectric $LiTaO_3$ (BVS = Li^{+} 0.793)[28] and $AgTaO_3$ (BVS = Ag^{+} 0.911)[30] are also under bonded.

On cooling below 938 K, $LiTaO_3$ undergoes a symmetry lowering distortion which leads to a change from the centrosymmetric, paraelectric structure (spacegroup $R\bar{3}c$) to a polar ferroelectric structure (spacegroup $R3c$) in which the lithium cations occupy only one of the two face-sharing "octahedral" A-cation sites and in which the Ta^{5+} cations are significantly displaced from the center of the TaO_6 octahedra, as shown in Figure 4.[31,32] The displacement of both the lithium and tantalum cations leads to a net spontaneous electrical polarization (ferroelectricity) in the material.

Refinement of noncentrosymmetric models analogous to the ferroelectric phase of $LiTaO_3$ (spacegroup P1) against neutron powder diffraction data collected from $Ni_{0.5}TaO_3$ at 5 and 298 K showed no evidence for an analogous ferroelectric distortion. Statistical fits using noncentrosymmetric models were no better than centrosymmetric models and atoms in $P1$ models refined to centrosymmetric arrangements within error, indicating an analogous symmetry-lowering structural distortion does not occur in $Ni_{0.5}TaO_3$. The observed centrosymmetric structure for $Ni_{0.5}TaO_3$ is supported by the lack of room temperature SHG activity observed for this phase.

The absence of a structural transition in $Ni_{0.5}TaO_3$ to a polar phase highlights the difficulties often encountered in preparing new ferroelectric materials. While local symmetry breaking distortions are often the primary driver for the adoption of polar structures, they do not guarantee such behavior. Nevertheless the formulation of $Ni_{0.5}TaO_3$ with a magnetic A-cation and an SOJT susceptible B-cation represents a novel route to multiferroic materials, which may yield useful materials in which magnetoelectric coupling is realized if a different combination of metal cations is used.

In a broader context, we believe that the redox-neutral, topochemical cation-exchange reaction used to prepare $Ni_{0.5}TaO_3$ is the first report of such a process being used to insert paramagnetic cations into a 3D cubic perovskite phase. Reductive cation insertion reactions, such as the intercalation of lithium into ReO_3 to form Li_xReO_3,[33,34] have been observed for 3D perovskite oxides, as has lithium/proton exchange in $LiTaO_3$ and $LiNbO_3$;[35] however, to the best of our knowledge, metal cation substitution reactions have to date been limited to layered perovskite structural variants, such as materials adopting Ruddlesden−Popper or Dion−Jacobson structures (see refs 18−20 for more comprehensive reviews of this area). The ability to bring about A-site cation exchange reactions in 3D perovskite phases opens up a synthetic route to a wide range of new metastable, A-site-substituted perovskite phases. This is particularly valuable if, as in the current case, paramagnetic cations can be introduced into the A-sites of perovskite lattices, as this allows elaborate magnetic materials to be prepared, such as materials with paramagnetic cations on both A- and B-sites. Furthermore, the topochemical nature of the cation exchange reactions allows a degree of rational synthesis and product targeting not normally available in the high-temperature, thermodynamically controlled conventional synthesis of complex oxide phases.

■ ASSOCIATED CONTENT

Ⓢ Supporting Information

Details of the drying procedure for $NiCl_2$. Selected bond lengths and angles from the refined structure of $Ni_{0.5}TaO_3$. Full details of the structural refinement of $Ni_{0.5}TaO_3$ at 5 K. This material is available free of charge via the Internet at http://pubs.acs.org.

■ AUTHOR INFORMATION

Corresponding Author

*E-mail: michael.hayward@chem.ox.ac.uk. Fax: +44 1865 272690. Tel.: +44 1865 272623.

Author Contributions

The manuscript was written through contributions of all authors.

Notes

The authors declare no competing financial interest.

■ ACKNOWLEDGMENTS

We thank E. Suard for assistance collecting the neutron diffraction data. M.A.P. thanks CONAYCT and the Balliol College, Oxford for a scholarship. W.Z. and P.S.H. thank the Welch Foundation (Grant E-1457) for support.

■ REFERENCES

(1) Hill, N. A. *J. Phys. Chem. B* **2000**, *104*, 6694.
(2) Halasyamani, P.; Poeppelmeier, K. R. *Chem. Mater.* **1998**, *10*, 2753.
(3) Cohen, R. E. *Nature* **1992**, *358*, 136.
(4) Kang, S. K.; Tang, H.; Albright, T. A. *J. Am. Chem. Soc.* **1993**, *115*, 1971.
(5) Kunz, M.; Brown, I. D. *J. Solid State Chem.* **1995**, *115*, 395.
(6) Pearson, R. G. *Theochem-Journal of Molecular Structure* **1983**, *12*, 25.
(7) Wheeler, R. A.; Whangbo, M. H.; Hughbanks, T.; Hoffmann, R.; Burdett, J. K.; Albright, T. A. *J. Am. Chem. Soc.* **1986**, *108*, 2222.
(8) Lefebvre, I.; Lannoo, M.; Allan, G.; Ibanez, A.; Fourcade, J.; Jumas, J. C.; Beaurepaire, E. *Phys. Rev. Lett.* **1987**, *59*, 2471.
(9) Lefebvre, I.; Szymanski, M. A.; Olivier-Fourcade, J.; Jumas, J. C. *Phys. Rev. B* **1998**, *58*, 1896.
(10) Seshadri, R.; Hill, N. A. *Chem. Mater.* **2001**, *13*, 2892.
(11) Stoltzfus, M. W.; Woodward, P. M.; Seshadri, R.; Klepeis, J. H.; Bursten, B. *Inorg. Chem.* **2007**, *46*, 3839.
(12) Watson, G. W.; Parker, S. C. *J. Phys. Chem. B* **1999**, *103*, 1258.
(13) Watson, G. W.; Parker, S. C.; Kresse, G. *Phys. Rev. B* **1999**, *59*, 8481.
(14) Catalan, G.; Scott, J. F. *Adv. Mater.* **2009**, *21*, 2463.
(15) Kimura, T.; Kawamoto, S.; Yamada, I.; Azuma, M.; Takano, M.; Tokura, Y. *Phys. Rev. B* **2003**, *67*, 180401.
(16) Seshadri, R.; Hill, N. A. *Chem. Mater.* **2001**, *13*, 2892.
(17) Wang, J.; Neaton, J. B.; Zheng, H.; Nagarajan, V.; Ogale, S. B.; Liu, B.; Viehland, D.; Vaithyanathan, V.; Schlom, D. G.; Waghmare, U. V.; Spaldin, N. A.; Rabe, K. M.; Wuttig, M.; Ramesh, R. *Science* **2003**, *299*, 1719.
(18) Schaak, R. E.; Mallouk, T. E. *Chem. Mater.* **2002**, *14*, 1455.
(19) Ranmohotti, K. G. S.; Josepha, E.; Choi, J.; Zhang, J. X.; Wiley, J. B. *Adv. Mater.* **2011**, *23*, 442.

(20) Hayward, M. A. In *Comprehensive Inorganic Chemistry II*; Reedijk, J., Poeppelmeier, K. R., Eds.; Elsevier: Oxford, 2013; Vol. 2, p 417.
(21) Hyeon, K. A.; Byeon, S. H. *Chem. Mater.* **1999**, *11*, 352.
(22) Ahtee, M.; Darlington, C. N. W. *Acta Crystallogr., Sect. B: Struct. Crystallogr. Cryst. Chem.* **1980**, *36*, 1007.
(23) Larson, A. C.; Von Dreele, R. B.; Los Alamos National Laboratory Report No. LAUR 86-748, 2000.
(24) Kurtz, S. K.; Perry, T. T. *J. Appl. Phys.* **1968**, *39*, 3798.
(25) Rieckhof, K. E.; Peticola, W. l. *Science* **1965**, *147*, 610.
(26) Ok, K. M.; Chi, E. O.; Halasyamani, P. S. *Chem. Soc. Rev.* **2006**, *35*, 710.
(27) Mullerbuschbaum, H.; Wichmann, R. *Z. Anorg. Allg. Chem.* **1986**, *536*, 15.
(28) Abrahams, S. C.; Buehler, E.; Hamilton, W. C.; Laplaca, S. J. *J. Phys. Chem. Solids* **1973**, *34*, 521.
(29) Shannon, R. D. *Acta Crystallogr.* **1976**, *A32*, 751.
(30) Wolcyrz, M.; Lukaszewski, M. *Zeitschrift Fur Kristallographie* **1986**, *177*, 53.
(31) Abrahams, S. C.; Bernstei, Jl *J. Phys. Chem. Solids* **1967**, *28*, 1685.
(32) Abrahams, S. C.; Hamilton, W. C.; Sequeira, A. *J. Phys. Chem. Solids* **1967**, *28*, 1693.
(33) Cava, R. J.; Santoro, A.; Murphy, D. W.; Zahurak, S.; Roth, R. S. *J. Solid State Chem.* **1982**, *42*, 251.
(34) Cava, R. J.; Santoro, A.; Murphy, D. W.; Zahurak, S. M.; Roth, R. S. *J. Solid State Chem.* **1983**, *50*, 121.
(35) Rice, C. E.; Jackel, J. L. *J. Solid State Chem.* **1982**, *41*, 308.